ЖЭТФ, 2025, том 167, вып. 5, стр. 626–634

ULTRAFAST LATTICE AND ELECTRON DYNAMICS INDUCED IN A PBSE CRYSTAL BY AN INTENSE TERAHERTZ PULSE

A. A. Melnikov [a*], ***Yu. G. Selivanov*** [b], ***D. G. Poydashev*** [a], ***S. V. Chekalin*** [a]

[a] *Institute for Spectroscopy, Russian Academy of Sciences*
108840, Troitsk, Moscow, Russia

[b] *P. N. Lebedev Physical Institute, Russian Academy of Sciences*
119991, Moscow, Russia

Received December 7, 2024
revised version December 7, 2024
Accepted for publication December 11, 2024

The ultrafast optical response of a PbSe crystal to an intense picosecond terahertz pulse with a peak electric field strength of up to ~ 500 kV/cm is studied. The reflectivity anisotropy signal contains oscillations at the fundamental frequency of the resonant infrared-active phonon mode as well as its second, third, and fourth harmonics. The effect is ascribed to coherent anharmonic phonons resonantly excited by the strong terahertz field. Pump terahertz pulses also induce an almost instantaneous Kerr effect and a long-lived optical anisotropy of the crystal with a characteristic decay time of $\gtrsim 100$ ps. We consider lattice distortion and phonon-assisted side valley population as possible origins of this metastable state.

DOI: 10.31857/S0044451025050025

1. INTRODUCTION

Lead selenide belongs to the family of monochalcogenides of lead, tin, and germanium with the formula MX, where M=Ge, Sn, Pb, and X=S, Se, Te. These solids possess a unique set of physical properties, among which is their very high thermoelectric efficiency caused by a favorable combination of relatively high carrier mobility and low thermal conductivity [1–6]. The latter, in turn, is a result of the peculiar lattice anharmonicity in these chalcogenides, whose mechanisms are actively studied [7–12]. Unusual anharmonic lattice effects observed in the MX crystals are often associated with the stereochemical activity of lone electron pairs of the cation M [13–16]. In cubic crystals these lone pairs induce shifts of cation atoms relative to their high-symmetry positions leading to the formation of fluctuating local dipoles and to lattice instability [8, 16–18]. The specific character of interatomic bonds in MX monochalcogenides also causes considerable anharmonicity of their transverse optical (TO) phonon modes. These modes are often actually the soft modes associated with a structural displacive phase transition [19–22]. Highly anharmonic TO phonons effectively scatter acoustic phonons, which carry heat, thereby lowering the thermal conductivity [7].

Transverse optical phonon modes in MX crystals have rather low frequencies in the terahertz range and are infrared-active. Now there exist nonlinear optical methods that allow efficient generation of picosecond terahertz pulses with high peak electric fields [23, 24]. Thus, it would be interesting to study ultrafast lattice dynamics induced via intense resonant excitation of coherent TO phonons.

Resonant pumping of infrared-active vibrations in solids by ultrashort laser pulses has emerged recently as a unique method for the ultrafast control of quantum materials and investigation of unusual nonequilibrium states [25–28]. A number of interesting concepts have already been demonstrated or suggested. In particular, it was shown that dipole-active atomic vibrations can couple quadratically to the electron density of a crystal, potentially enabling light-induced electronic phase transitions and superconductivity [29–34]. Anharmonic interactions of a highly-excited phonon mode can cause nonlinear lattice distortions and induce effective magnetic fields, providing a means of controlling the structural, ferroelectric, and magnetic order [35–43].

* E-mail: melnikov@isan.troitsk.ru

In our recent work we used intense terahertz pulses for resonant excitation of the soft TO phonon mode of a PbTe crystal and detected nonlinear atomic oscillations at frequencies up to the third harmonic of the fundamental frequency [44]. Relying on our data, it was also possible to assume that the terahertz electric field induces transient symmetry lowering accompanied by the short-lived polar order. The lattice of PbSe is often considered to be more anharmonic in comparison to that of PbTe [45]. Moreover, Pb-Se bonds have more "ionic" character, and, therefore, can demonstrate stronger coupling to the resonant terahertz radiation. In accordance with these assumptions, in the present work we have found that terahertz-driven anharmonic dynamics are more pronounced in PbSe and up to four harmonics of the TO phonon mode can be detected, which implies universality of these nonlinear lattice effects for lead monochalcogenides. Additionally, terahertz pulses induce a long-lived anisotropy of reflectivity of the PbSe crystal that we ascribe either to a metastable lattice distortion or to charge carriers transferred to the side valleys upon terahertz excitation. We have also detected a pronounced instantaneous terahertz electro-optic Kerr effect associated with a transient anisotropy of the electron distribution.

2. EXPERIMENTAL DETAILS

In our experiments we used nearly single-cycle picosecond terahertz pulses generated via optical rectification of femtosecond laser pulses with tilted fronts in a crystal of lithium niobate [46]. The description of the laser setup can be found in our previous publications [44]. The peak electric field of the focused ~ 1 ps terahertz pulses was up to ~ 500 kV/cm, while their peak frequency was near 1 THz (see Fig. *a* and *b*). The frequency of the infrared-active TO phonon mode in MX chalcogenides often depends considerably on carrier concentration N. In the case of soft modes, the frequency increases with N [47]. For PbTe and PbSe at room temperature it lies typically in the range of $\sim$ 0.8–1.0 THz and $\sim$ 1.3–1.5 THz, respectively [45, 47–51]. The crystal of PbSe that was studied in the present work was grown by the self-selecting vapor growth method adjusting the stoichiometric composition by adding a small amount of excess Se [52, 53]. The crystal was cleaved along the (100) plane. The room-temperature concentration of charge carriers was relatively low, $N \sim 5 \cdot 10^{18}$ cm^{-3} (p-type). Therefore, screening effects were expected to be moderate, allowing efficient excitation by resonant terahertz pulses.

In order to detect the optical response of the PbSe crystal to the pump terahertz pulse, we used weak femtosecond probe pulses at 800 nm. The pump and the probe beams were incident onto the sample at an angle of about 8°, while the initial polarization of the probe pulse was set to 45° relative to the vertical polarization of the pump terahertz pulses. Intensities of the vertical and horizontal polarization components of the reflected probe pulses I_y and I_x were detected using a Wollaston prism and a pair of amplified photodiodes. The measurement was repeated multiple times for open and closed pump beams (modulated by an optical chopper) and the normalized difference signal $S = 1 - (I_y^*/I_x^*)/(I_y/I_x)$ was calculated and then averaged (here the asterisk indicates intensities measured with the opened pump beam). For small angles of incidence $S \approx -4\varphi$, where φ is the rotation of polarization of the reflected probe pulse. In order to measure pump-induced changes of reflectivity, a similar procedure was performed, in which intensities of the reflected probe beam and of the reference beam were measured instead of intensities of the polarization components.

3. RESULTS AND DISCUSSION

Figure 1 *c* illustrates temporal evolution of the polarization rotation φ of the probe pulse reflected from the PbSe crystal that was measured in the experiment for crystal temperatures of 295 K and 90 K. The pump terahertz pulse arrives at approximately zero delay time ($t \sim 0$) and induces anisotropy of reflectivity of the sample, which reveals itself as the nonzero $\varphi(t)$ signal. The latter consists of damped oscillations superimposed onto a monotonic transient. At lower temperatures an additional pronounced waveform appears near $t \sim 0$ that is very similar to the squared terahertz electric field. In this time window the signal $\varphi(t)$ follows $E^2_{\mathrm{THz}}(t)$ almost instantaneously. Performing a convolution of the $E^2_{\mathrm{THz}}(t)$ function with a model exponential response, it is possible to roughly estimate the characteristic timescale of the underlying physical process as $\lesssim 100$ fs. Therefore, we ascribe this waveform to the quadratic electro-optic (Kerr) effect of the electronic origin. Moreover, we assume that this effect is determined by the intraband purely electronic processes. In this case its magnitude is expected to grow with increasing mobility of charge carriers. According to our results, at 90 K the Kerr effect is at least one order of magnitude larger than at room temperature (in fact, at 295 K it is indiscernible over the oscillations and noise). At the same time, the measured carrier

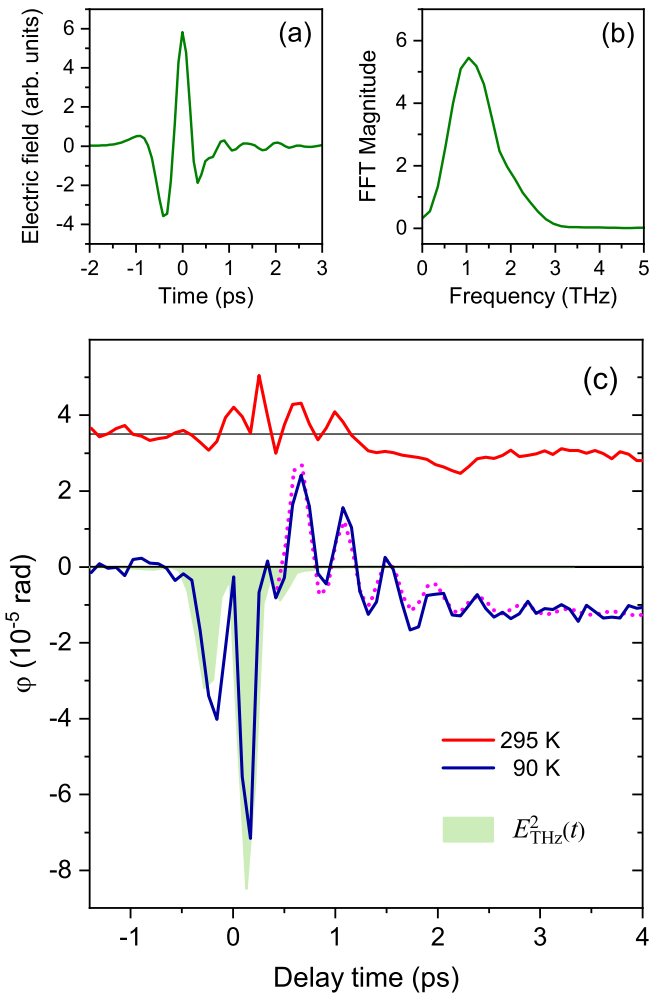

Fig. 1. *a* — Temporal profile of the pump terahertz pulse. *b* — Spectrum of the pulse shown in panel *a*. *c* — Polarization rotation φ of the probe pulse reflected from the PbSe crystal as a function of the pump-probe delay time measured at 295 K (red solid line) and at 90 K (blue solid line). The room-temperature curve is shifted up for clarity. Normalized squared electric field of the pump terahertz pulse in arbitrary units (green area). Pink dotted line illustrates the fit by Eq. (1) (see text)

mobility in our PbSe sample increases by a factor of ~ 12 upon cooling to 77 K.

The observation of the terahertz Kerr effect in PbSe is not a trivial fact. Indeed, the main intraband effect of the pump terahertz pulse on charge carriers is the Joule heating of the ensemble. If the electron-electron scattering rate is sufficiently high, a thermalized electron distribution will evolve during the pulse, the temperature of which approximately follows the integral of the squared electric field (provided the characteristic relaxation time of the electron temperature is rather long). This process reveals itself as transient changes of reflectivity, which should be isotropic, since PbSe has the centrosymmetric rock-salt structure and the electron distribution function as well as the electron-electron scattering processes are expected to be symmetric. However, these isotropic changes of reflectivity are cancelled out in the process of measurement of the $\varphi(t)$ signal. Therefore, the observed terahertz Kerr effect implies a small transient anisotropy of reflectivity that probably indicates a short-lived anisotropy of the electron distribution.

This counterintuitive result could in principle be explained by invoking the concept of local structural dipoles mentioned above. The dynamic local symmetry lowering caused by the off-centering of Pb cations implies breaking of the inversion symmetry and, therefore, can enable asymmetric scattering processes. One more mechanism should be also mentioned, which requires higher-order nonlinearity of the band dispersion.

It was proposed for doped semiconductors and metallic systems and is valid even for centrosymmetric crystals [54, 55]. Nevertheless, the detected terahertz Kerr effect in PbSe requires further studies, which are beyond the scope of the present work. In what follows, we will analyze the signal $\varphi(t)$ measured at 90 K starting from $t \sim 0.5$ ps, thereby excluding the Kerr waveform.

Next, we proceed to the discussion of the oscillations in the detected signal $\varphi(t)$. In femtosecond pump-probe experiments with nonmagnetic crystals, terahertz oscillations in the ultrafast optical response are usually associated with coherent atomic vibrations of certain symmetry (coherent phonons) induced by the pump pulses [56, 57]. For rock-salt PbSe crystals there are two phonon modes: TO mode at $\sim$ 1.3–1.5 THz and a longitudinal optical (LO) mode at $\sim$ 4 THz [45, 50, 51]. However, we rule out generation of coherent LO phonons of detectable amplitude by terahertz pulses. Indeed, in this case there is no resonance, while impulsive mechanisms are not effective, since the duration of the terahertz pulse ($\sim$ 1 ps) is considerably larger than the period of the LO phonon mode ($\sim$ 0.25 ps). We note that even for femtosecond pump pulses of relatively large fluence (0.5 mJ/cm^2 at 650 nm) we were unable to detect any oscillations in the $\varphi(t)$ response. We neglect also the sum-frequency Raman scattering of terahertz radiation [58], because in the absence of a resonant half-frequency vibrational transition this effect is expected to be very weak for the intensities of terahertz pulses used in our experiments [59,60]. Thus, in our case we expect only coherent excitation of the infrared-active TO mode by the resonant pump terahertz pulse.

Spectra of oscillations that are present in the $\varphi(t)$ transients measured at 295 K and 90 K are shown in Fig. 2. In both cases distinct bands appear near ω_{TO}, $2\omega_{\mathrm{TO}}$ and $3\omega_{\mathrm{TO}}$, where ω_{TO} is the fundamental frequency of the TO phonon mode of PbSe. The band at $3\omega_{\mathrm{TO}}$ in the room temperature spectrum is slightly shifted to higher frequencies probably due to interference with the shoulder of the broader band at $2\omega_{\mathrm{TO}}$ and/or an additional small contribution caused by the Kerr effect near zero delay time. For the low temperature spectrum, the correspondence is very good. It can be seen that as the fundamental frequency decreases upon cooling due to the softening of the TO mode, the second and third harmonics shift accordingly.

We ascribe this effect to nonlinear motion of the anharmonic oscillator associated with the TO phonon mode of PbSe, which is induced via resonant coherent

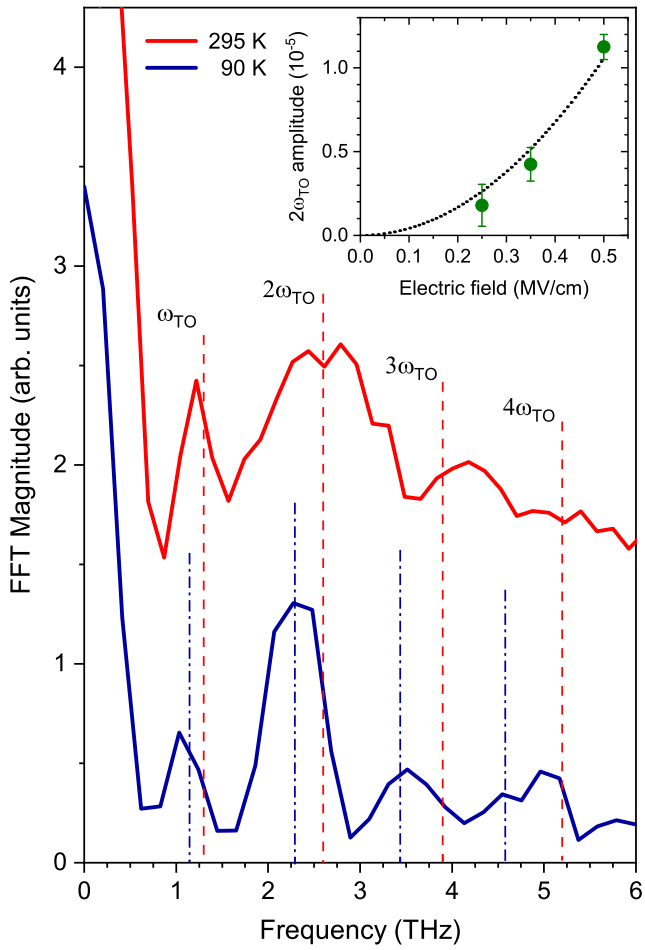

Fig. 2. Spectra of the oscillating components of the terahertz-induced signals $\varphi(t)$, measured at 295 K (red solid line) and 90 K (blue solid line). The room-temperature spectrum is shifted up for clarity. Vertical red dashed lines and blue dash-dotted lines indicate fundamental frequency of the TO mode as well as its harmonics at 295 K and 90 K, respectively. The $2\omega_{\mathrm{TO}}$ values are chosen as central frequencies of the most intense bands that correspond to the second harmonic. The ω_{TO}, $3\omega_{\mathrm{TO}}$ and $4\omega_{\mathrm{TO}}$ frequencies are then calculated from the $2\omega_{\mathrm{TO}}$ values. The inset shows the dependence of the amplitude of the second harmonic at $2\omega_{\mathrm{TO}}$ on the peak electric field strength of the terahertz pulse. Green circles — experimental values, dotted curve — a fit by a parabola $y = ax^2$

excitation by the intense terahertz pulse. A similar effect was observed in our previous work on PbTe [44], however, in that case only three harmonics were detected (red-shifted due to $\sim$ 30% lower frequency of the TO phonon mode of PbTe). For PbSe the harmonics are more pronounced already in the room temperature spectrum, while at 90 K an additional band near $4\omega_{\mathrm{TO}}$ appears, indicating contribution from the fourth harmonic.

An important question is how coherent infrared-active TO phonons become visible in the $\varphi(t)$ signal. Indeed, the detection scheme used in our experiments to measure $\varphi(t)$ is sensitive only to Raman active coherent phonons that cause anisotropic modulation of the refractive index of a crystal. However, for a perfect crystal with the rock-salt structure the first-order Raman scattering is forbidden [61, 62]. In our previous work on PbTe we suggested that these selection rules are lifted due to the short-lived lattice distortion induced by the terahertz pulse [44]. In this case, the apparent lifetime of the oscillations should be the same as the characteristic relaxation time of the fast monotonic component of $\varphi(t)$ that is associated with this distortion. In order to check this property for PbSe we fitted the $\varphi(t)$ trace detected at 90 K by the following function (excluding the Kerr waveform):

$$\varphi(t) = A_1 e^{(-t/\tau_1)} + A_2 e^{(-t/\tau_2)} \cos(2\pi\nu t + \phi) + \\ + A_3(e^{(-t/\tau_3)} - 1), \quad (1)$$

where ν is the frequency of the second harmonic $2\omega_{\mathrm{TO}}$ (here we include only oscillations with the highest amplitude), τ_1 and τ_2 are the decay times of the fast monotonic component and of the oscillations, respectively. The third term describes an additional long-lived component that appears with a delay. We have found that a satisfactory fit can be achieved if $\tau_1 \sim \tau_2 = 0.85 \pm 0.10$ ps and $A_1 \sim A_2$ in accordance with the above-mentioned hypothesis.

The short-lived lattice distortion can in principle be induced by the displacive force that is generated via "rectification" of the high-amplitude atomic vibrations of the TO mode due to the second-order lattice nonlinearity [35]. Then the relation $\tau_1 = \tau_2$ is naturally fulfilled. However, the mechanism of symmetry breaking for the initially centrosymmetric lattice is not clear in this case. Probably, it can be facilitated by the fluctuating local regions of lower symmetry typical for MX chalcogenides. One can consider also the electric field of the pump terahertz pulse acting on these local dipoles directly and producing a short-lived macroscopic "aligned" state lacking the center of inversion.

Besides the fast sub-picosecond monotonic component of the optical response of PbSe described by the first term in Eq. (1), we have detected a long-lived anisotropy of reflectivity that corresponds to the third term. It appears with a certain delay that is defined by the time τ_3, while its decay time T is so long that in our time window it can be treated as infinite (see Fig. 3 *a*). Taking into account the noise, it is possible

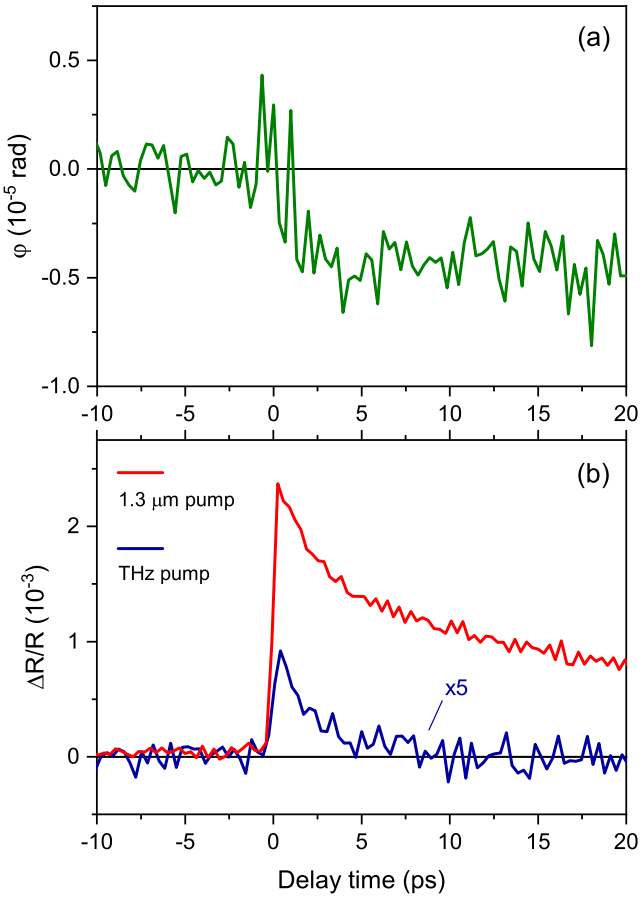

Fig. 3. *a* — Temporal evolution of the polarization rotation φ of the probe pulse in a broader time window. *b* — Transient changes of reflectivity of the PbSe crystal, induced by a femtosecond laser pulse with a central wavelength of 1300 nm (top red solid line, fluence ~ 0.3 mJ/cm^2) and by the terahertz laser pulse (blue solid line, the signal was multiplied by 5). All measurements were made at room temperature

to make a rough lower estimate of this time as $T \gtrsim 100$ ps. This long-lived anisotropy of reflectivity could be caused by a metastable distortion of the PbSe crystal lattice. However, this assumption would contradict the above interpretation, according to which the nonequilibrium lattice state of lower symmetry exists only during ~ 1 ps. It is possible to consider also the electronic origin of the long-lived component. Here, we can exclude intraband processes. Indeed, as we discussed above, the anisotropy of the electron distribution that likely causes the terahertz Kerr effect has a lifetime of $\lesssim 100$ fs. Cooling of the charge carriers heated by the terahertz pulse occurs with a characteristic time of ~ 3 ps, as can be inferred from the kinetics of transient isotropic reflectivity changes (see Fig. 3 *b*). Sufficiently longer decay times can be expected only

in the case of interband excitation (cf. the kinetics of reflectivity changes induced by a femtosecond pulse at 1300 nm, Fig. 3 *b*). However, for the terahertz pump pulses used in our experiments the probability of direct interband transitions (via multiphoton processes or tunneling) is expected to be very low taking into account the ~ 0.26 eV band gap of PbSe. Nevertheless, it is possible to consider the hole transfer between L and Σ valleys, since in p-type PbSe the Fermi level can lie rather close to the top of the Σ valley [63–66]. In this case, the population of Σ-valley states by holes could induce anisotropy of reflectivity via polarization-sensitive selection rules, if allowed by symmetry. Surprisingly, the rise time of the long-lived component $\tau_3 = 0.75 \pm 0.25$ ps, which is close to the decay time of the hypothetical transient lattice distortion τ_1 and to the decay time of the second harmonic oscillations τ_2. This fact implies that such intervalley hole transfer could be promoted by intense coherent atomic vibrations rather than by the terahertz field itself.

4. CONCLUSION

In conclusion, we have found that intense terahertz pulses generate anharmonic coherent atomic vibrations in PbSe via resonant excitation of the TO phonon mode of the crystal. We have detected the second, the third, and the fourth harmonic of the fundamental frequency in the spectrum of these oscillations. In general, nonlinear lattice dynamics in PbSe were found to be more pronounced compared to the case of PbTe that we studied earlier. Moreover, terahertz electric field induces in PbSe a nearly instantaneous electro-optic Kerr effect, indicating transient anisotropy of electron distribution. Terahertz excitation also results in a long-lived anisotropy of reflectivity of the PbSe crystal that can be associated with a metastable lattice distortion or with charge carriers promoted to the side valleys. Our results suggest universality of the observed terahertz-driven nonlinear lattice effects for lead monochalcogenides. Excitation of infrared-active TO phonons by intense terahertz pulses can be used to create unusual highly nonequilibrium lattice states in other monochalcogenides of germanium, tin, and lead in order to study lattice anharmonicity, dynamics of polar order in the presence of charge carriers, as well as the nonlinear electron-phonon interaction.

Funding. The reported study was funded by the Russian Science Foundation, Project No. 23-22-00387.

REFERENCES

1. J. He and T. M. Tritt, *Advances in Thermoelectric Materials Research: Looking Back and Moving Forward*, Science **357**, eaak9997 (2017).

2. J. Wei, L. Yang, Z. Ma, P. Song, M. Zhang, J. Ma, F. Yang, and X. Wang, *Review of Current High-ZT Thermoelectric Materials*, J. Mater. Sci. **55**, 12642 (2020).

3. Z. Hu, Y. Ding, X. Hu, W. Zhou, X. Yu, and S. Zhang, *Recent Progress in 2D Group IV-IV Monochalcogenides: Synthesis, Properties and Applications*, Nanotechnology **30**, 252001 (2019).

4. A. Shafique and Y.-H. Shin, *Thermoelectric and Phonon Transport Properties of Two-Dimensional IV-VI Compounds*, Sci. Rep. **7**, 506 (2017).

5. A. N. Filanovich and A. A. Povzner, *Phonon Spectra and Lattice Thermal Conductivity of High-Performance Thermoelectric SnSe*, JETP Lett. **120**, 195 (2024).

6. A. S. Starkov and I. A. Starkov, *Averaging of Thermoelectric Media: Thermoelectric Potential Distribution*, JETP **134**, 211 (2022).

7. O. Delaire, J. Ma, K. Marty, A. F. May, M. A. McGuire, M.-H. Du, D. J. Singh, A. Podlesnyak, G. Ehlers, M. D. Lumsden, and B. C. Sales, *Giant Anharmonic Phonon Scattering in PbTe*, Nat. Mater. **10**, 614 (2011).

8. M. P. Jiang, M. Trigo, I. Savić, S. Fahy, É. D. Murray, C. Bray, J. Clark, T. Henighan, M. Kozina, M. Chollet, J. M. Glownia, M. C. Hoffmann, D. Zhu, O. Delaire, A. F. May, B. C. Sales, A. M. Lindenberg, P. Zalden, T. Sato, R. Merlin, and D. A. Reis, *The Origin of Incipient Ferroelectricity in Lead Telluride*, Nat. Commun. **7**, 12291 (2016).

9. C. W. Li, J. Hong, A. F. May, D. Bansal, S. Chi, T. Hong, G. Ehlers, and O. Delaire, *Orbitally Driven Giant Phonon Anharmonicity in SnSe*, Nat. Phys. **11**, 1063 (2015).

10. T. Lanigan-Atkins, S. Yang, J. L. Niedziela, D. Bansal, A. F. May, A. A. Puretzky, J. Y. Y. Lin, D. M. Pajerowski, T. Hong, S. Chi, G. Ehlers, and O. Delaire, *Extended Anharmonic Collapse of Phonon Dispersions in SnS and SnSe*, Nat. Commun. **11**, 4430 (2020).

11. J. M. Skelton, L. A. Burton, S. C. Parker, A. Walsh, C.-E. Kim, A. Soon, J. Buckeridge, A. A. Sokol,

C. Richard A. Catlow, A. Togo, and I. Tanaka, *Anharmonicity in the High-Temperature Cmcm Phase of SnSe: Soft Modes and Three-Phonon Interactions*, Phys. Rev. Lett. **117**, 075502 (2016).

12. S. A. J. Kimber, J. Zhang, C. H. Liang, G. G. Guzman-Verri, P. B. Littlewood, Y. Cheng, D. L. Abernathy, J. M. Hudspeth, Z.-Z. Luo, M. G. Kanatzidis, T. Chatterji, A. J. Ramirez-Cuesta, and S. J. L. Billinge, *Dynamic Crystallography Reveals Spontaneous Anisotropy in Cubic GeTe*, Nat. Mater. **22**, 311 (2023).

13. U. V. Waghmare, N. A. Spaldin, H. C. Kandpal, and R. Seshadri, *First-Principles Indicators of Metallicity and Cation Off-Centricity in the IV-VI Rocksalt Chalcogenides of Divalent Ge, Sn, and Pb*, Phys. Rev. B **67**, 125111 (2003).

14. A. Walsh and G. W. Watson, *The Origin of the Stereochemically Active Pb(II) Lone Pair: DFT Calculations on PbO and PbS*, J. Solid State Chem. **178**, 1422 (2005).

15. M. D. Nielsen, V. Ozolins, and J. P. Heremans, *Lone Pair Electrons Minimize Lattice Thermal Conductivity*, Energy Environ. Sci. **6**, 570 (2013).

16. B. Sangiorgio, E. S. Božin, C. D. Malliakas, M. Fechner, A. Simonov, M. G. Kanatzidis, S. J. L. Billinge, N. A. Spaldin, and T. Weber, *Correlated Local Dipoles in PbTe*, Phys. Rev. Materials **2**, 085402 (2018).

17. E. S. Božin, C. D. Malliakas, P. Souvatzis, T. Proffen, N. A. Spaldin, M. G. Kanatzidis, and S. J. L. Billinge, *Entropically Stabilized Local Dipole Formation in Lead Chalcogenides*, Science **330**, 1660 (2010).

18. K. M. Ø. Jensen, E. S. Božin, C. D. Malliakas, M. B. Stone, M. D. Lumsden, M. G. Kanatzidis, S. M. Shapiro, and S. J. L. Billinge, *Lattice Dynamics Reveals a Local Symmetry Breaking in the Emergent Dipole Phase of PbTe*, Phys. Rev. B **86**, 085313 (2012).

19. M. Iizumi, Y. Hamaguchi, K. F. Komatsubara, and Y. Kato, *Phase Transition in SnTe With Low Carrier Concentration*, J. Phys. Soc. Jpn. **38**, 443 (1975).

20. C. Wang, J. Wu, Z. Zeng, J. Embs, Y. Pei, J. Ma, and Y. Chen, *Soft-Mode Dynamics in the Ferroelectric Phase Transition of GeTe*, npj Comput. Mater. **7**, 118 (2021).

21. Y. Huang, S. Teitelbaum, S. Yang, G. De la Pena, T. Sato, M. Chollet, D. Zhu, J. L. Niedziela, D. Bansal, A. F. May, A. M. Lindenberg, O. Delaire, M. Trigo, and D. A. Reis, *Nonthermal Bonding Origin of a Novel Photoexcited Lattice Instability in SnSe*, Phys. Rev. Lett. **131**, 156902 (2023).

22. J. Shi, W. You, X. Li, F. Y. Gao, X. Peng, S. Zhang, J. Li, Y. Zhang, L. Fu, P. J. Taylor, K. A. Nelson, and E. Baldini, *Revealing a Distortive Polar Order Buried in the Fermi Sea*, Sci. Adv. **10**, eadn0929 (2024).

23. J. A. Fülöp, S. Tzortzakis, and T. Kampfrath, *Laser-Driven Strong-Field Terahertz Sources*, Adv. Optical Mater. **8**, 1900681 (2020).

24. B. V. Rumiantsev, A. V. Pushkin, D. Z. Suleimanova, N. A. Zhidovtsev, and F. V. Potemkin, *Generation of Intense Few-Cycle Terahertz Radiation in Organic Crystals Pumped by 1.24-μm Multigigawatt Chirped Laser Pulses*, JETP Lett. **117**, 566 (2023).

25. T. Kampfrath, K. Tanaka, and K. A. Nelson, *Resonant and Nonresonant Control Over Matter and Light by Intense Terahertz Transients*, Nat. Photonics **7**, 680 (2013).

26. D. Nicoletti and A. Cavalleri, *Nonlinear Light-Matter Interaction at Terahertz Frequencies*, Adv. Opt. Photonics **8**, 401 (2016).

27. D. N. Basov, R. D. Averitt and D. Hsieh, *Towards Properties on Demand in Quantum Materials*, Nat. Materials **16**, 1077 (2017).

28. H. Hübener, U. De Giovannini, and A. Rubio, *Phonon Driven Floquet Matter*, Nano Lett. **18**, 1535 (2018).

29. I. Gierz, M. Mitrano, H. Bromberger, C. Cacho, R. Chapman, E. Springate, S. Link, U. Starke, B. Sachs, M. Eckstein, T. O. Wehling, M. I. Katsnelson, A. Lichtenstein, and A. Cavalleri, *Phonon-Pump Extreme-Ultraviolet-Photoemission Probe in Graphene: Anomalous Heating of Dirac Carriers by Lattice Deformation*, Phys. Rev. Lett. **114**, 125503 (2015).

30. D. M. Kennes, E. Y. Wilner, D. R. Reichman, and A. J. Millis, *Transient Superconductivity From Electronic Squeezing of Optically Pumped Phonons*, Nat. Phys. **13**, 479 (2017).

31. M. A. Sentef, *Light-Enhanced Electron-Phonon Coupling From Nonlinear Electron-Phonon Coupling*, Phys. Rev. B **95**, 205111 (2017).

32. M. Mitrano, A. Cantaluppi, D. Nicoletti, S. Kaiser, A. Perucchi, S. Lupi, P. Di Pietro, D. Pontiroli, M. Ricco, S. R. Clark, D. Jaksch, and A. Cavalleri, *Possible Light-Induced Superconductivity in K_3C_{60} at High Temperature*, Nature **530**, 461 (2016).

33. M. Rini, R. Tobey, N. Dean, J. Itatani, Y. Tomioka, Y. Tokura, R. W. Schoenlein, and A. Cavalleri, *Control of the Electronic Phase of a Manganite by Mode-Selective Vibrational Excitation*, Nature **449**, 72 (2007).

34. V. Esposito, M. Fechner, R. Mankowsky, H. Lemke, M. Chollet, J. M. Glownia, M. Nakamura, M. Kawasaki, Y. Tokura, U. Staub, P. Beaud, and M. Först, *Nonlinear Electron-Phonon Coupling in Doped Manganites*, Phys. Rev. Lett. **118**, 247601 (2017).

35. M. Först, C. Manzoni, S. Kaiser, Y. Tomioka, Y. Tokura, R. Merlin, and A. Cavalleri, *Nonlinear Phononics as an Ultrafast Route to Lattice Control*, Nat. Phys. **7**, 854 (2011).

36. A. Subedi, *Proposal for Ultrafast Switching of Ferroelectrics Using Midinfrared Pulses*, Phys. Rev. B **92**, 214303 (2015).

37. D. M. Juraschek, M. Fechner, and N. A. Spaldin, *Ultrafast Structure Switching Through Nonlinear Phononics*, Phys. Rev. Lett. **118**, 054101 (2017).

38. A. von Hoegen, R. Mankowsky, M. Fechner, M. Först, and A. Cavalleri, *Probing the Interatomic Potential of Solids With Strong-Field Nonlinear Phononics*, Nature **555**, 79 (2018).

39. M. Fechner, A. Sukhov, L. Chotorlishvili, C. Kenel, J. Berakdar, and N. A. Spaldin, *Magnetophononics: Ultrafast Spin Control Through the Lattice*, Phys. Rev. Materials **2**, 064401 (2018).

40. X. Li, T. Qiu, J. Zhang, E. Baldini, J. Lu, A. M. Rappe, and K. A. Nelson, *Terahertz Field-Induced Ferroelectricity in Quantum Paraelectric $SrTiO_3$*, Science **364**, 1079 (2019).

41. T. F. Nova, A. S. Disa, M. Fechner, and A. Cavalleri, *Metastable Ferroelectricity in Optically Strained $SrTiO_3$*, Science **364**, 1075 (2019).

42. A. A. Melnikov, Yu. G. Selivanov, and S. V. Chekalin, *Phonon-Driven Ultrafast Symmetry Lowering in a Bi_2Se_3 Crystal*, Phys. Rev. B **102**, 224301 (2020).

43. A. A. Melnikov, K. N. Boldyrev, Yu. G. Selivanov, and S. V. Chekalin, *Anomalous Behavior of the Infrared-Active Phonon Mode in $Bi_{2-x}Sr_xSe_3$ Crystal*, JETP Lett. **115**, 34 (2022).

44. A. A. Melnikov, Yu. G. Selivanov, and S. V. Chekalin, *Anharmonic Coherent Dynamics of the Soft Phonon Mode of a PbTe Crystal*, Phys. Rev. B **108**, 224309 (2023).

45. Z. Tian, J. Garg, K. Esfarjani, T. Shiga, J. Shiomi, and G. Chen, *Phonon Conduction in PbSe, PbTe, and $PbTe_{1-x}Se_x$ From First-Principles Calculations*, Phys. Rev. B **85**, 184303 (2012).

46. A. G. Stepanov, J. Hebling, and J. Kuhl, *Efficient Generation of Subpicosecond Terahertz Radiation by Phase-Matched Optical Rectification Using Ultrashort Laser Pulses With Tilted Pulse Fronts*, Appl. Phys. Lett. **83**, 3000 (2003).

47. H. Burkhard, G. Bauer, and A. Lopez-Otero, *Submillimeter Spectroscopy of TO-Phonon Mode Softening in PbTe*, J. Opt. Soc. Am. **67**, 943 (1977).

48. W. Cochran, R. A. Cowley, G. Dolling, and M. M. Elcombe, *The Crystal Dynamics of Lead Telluride*, Proc. R. Soc. Lond. A **293**, 433 (1966).

49. H. A. Alperin, S. J. Pickart, J. J. Rhyne, and V. J. Minkiewicz, *Softening of the Transverse-Optic Mode in PbTe*, Phys. Lett. A **40**, 295 (1972).

50. *Lead Selenide (PbSe) Phonon Frequencies, Sound Velocities*, in *Landolt-Börnstein – Group III Condensed Matter 41C (Non-Tetrahedrally Bonded Elements and Binary Compounds I)*, ed. by O. Madelung, U. Rössler, and M. Schulz Springer-Verlag, Berlin–Heidelberg (1998).

51. J. Chen and W. Z. Shen, *Raman Study of Phonon Modes and Disorder Effects in $Pb_{1-X}Sr_xSe$ Alloys Grown by Molecular Beam Epitaxy*, J. Appl. Phys. **99**, 013513 (2006).

52. H. Maier, D. R. Daniel, and H. Preier, *Sublimation Growth of PbSe Crystals With Controlled Carrier Concentration*, J. Cryst. Growth **35**, 121 (1976).

53. A. Szczerbakow and K. Durose, *Self-Selecting Vapour Growth of Bulk Crystals — Principles and Applicability*, Progr. Cryst. Growth Mater. **51**, 81 (2005).

54. D. Ma, Y. Xiong, and J. C. W. Song, *Skew-Scattering Pockels Effect and Metallic Electro-Optics in Gapped Bilayer Graphene*, arXiv:2407.12096v1.

55. L. A. Almasov and I. M. Dykman, *High-Frequency Conductivity of Hot Carriers in Semiconductors With Non-Parabolic Dispersion Law of Energy*, Phys. Status Solidi B **48**, 563 (1971).

56. T. Dekorsy, G. C. Cho, and H. Kurz, *Coherent Phonons in Condensed Media*, in *Light Scattering in Solids VIII*, ed. by M. Cardona and G. Guntherodt, Springer, Berlin (2000), Chap. 4, p. 169.

57. O. V. Misochko, *Coherent Phonons and Their Properties*, JETP **92**, 246 (2001).

58. S. Maehrlein, A. Paarmann, M. Wolf, and T. Kampfrath, *Terahertz Sum-Frequency Excitation of a Raman-Active Phonon*, Phys. Rev. Lett. **119**, 127402 (2017).

59. D. M. Juraschek and S. F. Maehrlein, *Sum-Frequency Ionic Raman Scattering*, Phys. Rev. B **97**, 174302 (2018).

60. A. A. Melnikov, K. N. Boldyrev, Yu. G. Selivanov, V. P. Martovitskii, S. V. Chekalin, and E. A. Ryabov, *Coherent Phonons in a Bi_2Se_3 Film Generated by an Intense Single-Cycle THz Pulse*, Phys. Rev. B **97**, 214304 (2018).

61. M. Born and M. Bradburn, *The Theory of the Raman Effect in Crystals, in Particular Rock-Salt*, Proc. R. Soc. A **188**, 161 (1947).

62. J. R. Ferraro, *Factor Group Analysis for Some Common Minerals*, Appl. Spectrosc. **29**, 418 (1975).

63. F. Herman, R. L. Kortum, I. B. Ortenburger, and J. P. Van Dyke, *Relativistic Band Structure of GeTe, SnTe, PbTe, PbSe, and PbS*, J. Phys. Colloques **29**, C4-62 (1968).

64. J. Xin, Y. Tang, Y. Liu, X. Zhao, H. Pan, and T. Zhu, *Valleytronics in Thermoelectric Materials*, npj Quant. Mater. **3**, 9 (2018).

65. R. D'Souza, J. Cao, J. D. Querales-Flores, S. Fahy, and I. Savić, *Electron-Phonon Scattering and Thermoelectric Transport in p-Type PbTe From First Principles*, Phys. Rev. B **102**, 115204 (2020).

66. Y. Zhu, D. Wang, T. Hong, L. Hu, T. Ina, S. Zhan, B. Qin, H. Shi, L. Su, X. Gao, and L.-D. Zhao, *Multiple Valence Bands Convergence and Strong Phonon Scattering Lead to High Thermoelectric Performance in p-Type PbSe*, Nat. Commun. **13**, 4179 (2022).